発表者氏名	論文タイトル名	発表誌名	巻号	ページ	出版年
Narumi Y, Shiihara T, others, Matsumoto N, Fukushima Y.	Hypomyelination with atrophy of the basal ganglia and cerebellum (H-ABC) in an infant with Down syndrome.	Clin Dysmorphol	20 (3)	166-167	2011
Saitsu H, Matsumoto N.	Genetic commentary: *De novo* mutations in epilepsy.	Dev Med Child Neurol	53 (9)	806-807	2011

SHORT REPORT

Rapid detection of a mutation causing X-linked leucoencephalopathy by exome sequencing

Yoshinori Tsurusaki,[1] Hitoshi Osaka,[2] Haruka Hamanoue,[1] Hiroko Shimbo,[2] Megumi Tsuji,[2] Hiroshi Doi,[1] Hirotomo Saitsu,[1] Naomichi Matsumoto,[1] Noriko Miyake[1]

[1]Department of Human Genetics, Yokohama City University Graduate School of Medicine, Yokohama, Japan
[2]Division of Neurology, Clinical Research Institute, Kanagawa Children's Medical Center, Yokohama, Japan

Correspondence to
Dr Noriko Miyake, Department of Human Genetics, Yokohama City University Graduate School of Medicine, 3-9 Fukuura, Kanazawa-ku, Yokohama 236-0004, Japan;
nmiyake@yokohama-cu.ac.jp

Received 20 October 2010
Revised 14 December 2010
Accepted 5 February 2011
Published Online First
17 March 2011

ABSTRACT

Background Conventional PCR-based direct sequencing of candidate genes for a family with X-linked leucoencephalopathy with unknown aetiology failed to identify any causative mutations.

Objective To carry out exome sequencing of entire transcripts of the whole X chromosome to investigate a family with X linked leucoencephalopathy.

Methods and results Next-generation sequencing of all the transcripts of the X chromosome, after liquid-based genome partitioning, was performed on one of the two affected male subjects (the proband) and an unaffected male subject (his brother). A nonsense mutation in *MCT8* (c.1102A→T (p.R368X)) was identified in the proband. Subsequent PCR-based direct sequencing of other family members confirmed the presence of this mutation, hemizygous in the other affected brother and heterozygous in the proband's mother and maternal grandmother. *MCT8* mutations usually cause abnormal thyroid function in addition to neurological abnormalities, but this proband had normal thyroid function.

Conclusion Single-lane exome next-generation sequencing is sufficient to fully analyse all the transcripts of the X chromosome. This method is particularly suitable for mutation screening of X-linked recessive disorders and can avoid biases in candidate gene choice.

INTRODUCTION

High-throughput, next-generation sequencing (NGS) can have a tremendous impact on human genetic research.[1] Even personal whole-genome analysis is possible,[2] but the cost of obtaining and analysing an entire genome from many people is still unrealistic for many laboratories. Selection and enrichment of regions of interest (genome partitioning) enable us to use NGS efficiently for reasonable numbers of patients with genetic disorders.[3–6]

Ready-to-use microarray-based and solution-based hybridisation systems are now commercially available. A combination of genome partitioning using these systems and NGS is one of the most promising ways to identify genes causing Mendelian disorders.[3 4 6]

Here, we performed exome sequencing of entire transcripts of the whole X chromosome to investigate a family with X linked leucoencephalopathy with unknown aetiology after intensive candidate gene analysis by conventional exon-by-exon Sanger sequencing. A single-lane run of NGS on only two family members successfully determined the leucoencephalopathy-causing mutation.

SUBJECTS AND METHODS

A family with X-linked leucoencephalopathy

The proband (III-2) was a 13-year-old boy. He was born to Japanese consanguineous parents (II-3, 4) after an uneventful pregnancy (figure 1A). His birth weight was 3440 g. Congenital horizontal nystagmus was noted as a neonate. Because of his poor weight gain and developmental delay, he was referred to us at age 5 months. He showed progressive spasticity and dystonia with exaggerated deep tendon reflexes as well as myoclonic and tonic seizures, which responded to valproic acid and clonazepam at age 21 months. Brain MRI at 2 years showed diffuse hyperintensity of the frontal lobe on T2-weighted images, suggesting hypomyelination, and normal T1-weighted images (figure 1B,C). The peak latency intervals in auditory brainstem responses (I–V/III–V) were 4.63/2.37 ms, which were elongated compared with those of age-matched controls (4.24±0.08/1.97±0.08 ms (mean±SD)). He was clinically diagnosed with Pelizaeus–Merzbacher disease (MIM#312080), although neither mutation nor duplication was found in *PLP1* (RefSeq Gene ID, NM_000533) or *GJA12* (NM_020435) (the duplication in *GJA12* was not checked). He was never able to follow objects or control his head.

The dystonia worsened and he is now mechanically ventilated because of tracheomalacia. A thyroid function test at age 13 years indicated all normal levels: free tri-iodothyronine (T_3) 1.2 ng/ml (normal range 0.8–1.6 ng/ml), free thyroxine (T_4) 6.4 μg/dl (normal range 6.1–12.4 μg/dl) and thyroid-stimulating hormone 1.2 μIU/ml (normal range 0.5–5 μIU/ml). Brain MRI at age 13 years demonstrated improvement of myelination in the white matter, but he still presented with severe mental retardation (figure 1D,E). His younger brother was an 8-year-old boy (III-3) with an almost identical clinical course and MRI findings. His grandparents (I-1, I-2) were both healthy. The elder uncle (II-1) died at age 27 years who, initially, could walk with support but who declined towards the end of his life. Another uncle (II-2) was diagnosed with cerebral palsy and died at 7 months of age of unknown causes.

Informed consent was obtained from the patient's family members in accordance with human study protocols approved by the

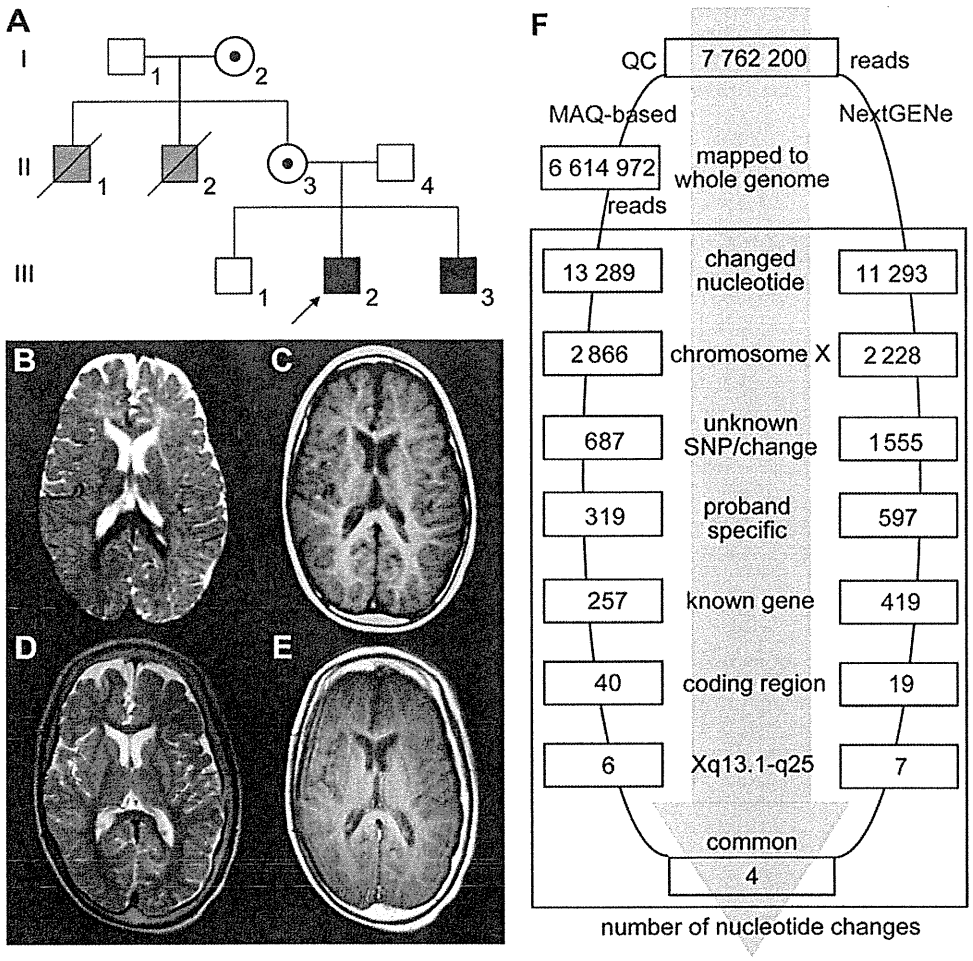

Figure 1 Pedigree and brain MRI of the proband. (A) Family pedigree. (B) T2-weighted image at age 2 years shows diffuse hyperintensity, especially in the frontal lobe. (C) T1-weighted image at 2 years shows nearly complete myelination. (D and E) At age 13 years, both T2 (D) and T1 (E)-weighted images demonstrate complete myelination; the hypomyelination observed at age 2 years can therefore be regarded as delayed myelination. (F) Flow of informatics analysis. A MAQ-based method and NextGENe analysis were performed (III-2). The selection methods included variation relative to the human genome reference sequence; variants mapped to the X chromosome; unknown variants (excluding registered SNPs); variants identified in the proband only (not in his healthy brother); variants in known genes; coding region variants; variants in genes at Xq13.1–q25; and variants common to the two informatics methods. MAQ, Mapping and Assembly with Qualities; SNP, single nucleotide polymorphism.

institutional review board at Kanagawa Children's Medical Centre and Yokohama City University School of Medicine.

Genome-wide single nucleotide polymorphism (SNP) genotyping

Genome-wide SNP genotyping was undertaken for individuals I-1, I-2, II-3, II-4, III-1, III-2 and III-3 using the GeneChip Human Mapping 10K Array *Xba* 142 2.0 (Affymetrix Inc, Santa Clara, California, USA), according to the manufacturer's protocols. Mendelian errors in the pedigree to exclude conflicted SNPs were checked using GeneChip operating software 1.2 (Affymetrix) and batch analysis in GeneChip genotyping analysis software 4.0 (Affymetrix), with the default settings for a mapping algorithm. Copy Number Analyzer for GeneChip 2.0 was used to validate copy number alterations.[7] The linked region with SNPs shared between individuals III-2 and III-3 (not observed in III-1) was checked manually.

Genome partitioning, short-read sequencing and sequence alignment

Genomic DNAs from the proband (III-2) and his unaffected brother (III-1) were used for this study. Three micrograms of DNA were processed using a SureSelect X chromosome test kit (1582 transcripts covering 3053 kb) (Agilent Technologies, Santa Clara, California, USA), according to the manufacturer's instructions. Captured DNAs were analysed using an Illumina GAIIx (Illumina Inc, San Diego, California, USA). We used only one of the eight lanes of the flow cell (Illumina), performing single 76 bp reads for each sample. Image analysis and base calling were performed by sequence control software (SCS) real-time analysis (Illumina) and/or offline Basecaller software v1.6 (Illumina) and CASAVA software v1.6 (Illumina). Reads were aligned to the human reference genome sequence (UCSC hg18, NCBI build 36.1) using the ELAND v2 program (Illumina). Coverage was calculated statistically. Identified variants were annotated based on novelty, impact on the encoded protein, the number and frequency of reads and conservation. NextGENe software v1.99 (SoftGenetics, State College, Pennsylvania, USA) was also used to analyse reads, with the default settings.

Mapping strategy and variant annotation

Approximately 9.9 million reads from III-1 (the unaffected sibling) and 7.8 million reads from III-2 (the proband), which passed the quality control (Path Filter), were mapped to the human reference genome by Mapping and Assembly with Qualities (MAQ)[8] and NextGENe software (SoftGenetics) (figure 1F). The bait region of the X chromosome based on the manufacturer's information was carefully evaluated. MAQ was able to align 7 359 688 and 6 614 972 reads to the whole genome for III-1 and III-2, respectively, which were statistically analysed for coverage using a script created by BITS Co Ltd (Tokyo, Japan). SNPs and indels were extracted from the alignment data using another script created by BITS, along with information on registered SNPs (dbSNP build 130). A consensus quality score of ≥40 was used for the SNP analysis in MAQ.

Capillary sequencing

Possible pathological variants were confirmed by Sanger sequencing using an ABI 3500xl or ABI3100 autosequencer (Life Technologies, Carlsbad, California, USA), following the manufacturer's protocol. Sequencing data were analysed by

Sequencher software (Gene Codes Corporation, Ann Arbor, Michigan, USA).

RESULTS AND DISCUSSION

Coverage analysis showed that 78.9% of all the X chromosome transcripts were completely covered by reads, and that 11.6% of transcripts were at least 90% covered. Almost all (99%) of these regions were covered by 20 reads or more (100 reads or more in 97%) by only single-lane sequencing. SNP genotyping was able to delineate the minimal linked region from rs763739 to rs1073455 (UCSC genome browser hg19 assembly, X chromosome coordinates: 76 804 990–126 844 262) (50 Mb). The maximum linked region was from rs1926354 to rs859587 (UCSC genome browser coordinates: 68 404 915–128 933 907) (60.5 Mb). Exome GAIIx sequencing with the two informatics methods identified four potentially interesting changes in the maximum linked region: c.1102AT (p.R368X) in *MCT8* (NM_006517; alternatively called *SLC16A2*); c.1402T→G (p.S468A) and c.1943A→G (p.H648R) in *CYLC1* (NM_021118); and c1606G→A (p.D536N) in *LRCH2* (NM_020871) (figure 1F). c.1102A→T (p.R368X) in *MCT8* was found heterozygously in the proband's healthy mother (II-3) and maternal grandmother (I-2), and hemizygously in the proband and his affected younger brother; each was confirmed by Sanger sequencing (figure 2). This change was not present among 92 normal female controls (0/184 alleles).

The *MCT8* gene encodes a thyroid hormone transporter and is implicated in syndromic X-linked mental retardation, Allan–Herndon–Dudley syndrome and Pelizaeus–Merzbacher-like disease (PMLD).[9–12] This nonsense mutation, c.1102A→T (p.R368X), which might lead to nonsense-mediated decay resulting in no protein production, is highly likely to be pathological. Based on the human gene mutation database (http://www.hgmd.cf.ac.uk/ac/index.php), three nonsense mutations in this gene have been previously registered: p.R245X, p.Q335X and p.S448X. The other identified variants, in *CYLC1* and *LRCH2*, are all SNPs because they were identified in normal controls: c.1402T→G (*CYLC1*): 5/182 alleles, c.1943A→G (*CYLC1*): 12/184 alleles and c1606G→A (*LRCH2*): 5/184 alleles. We concluded that the *MCT8* mutation was pathogenic in this family.

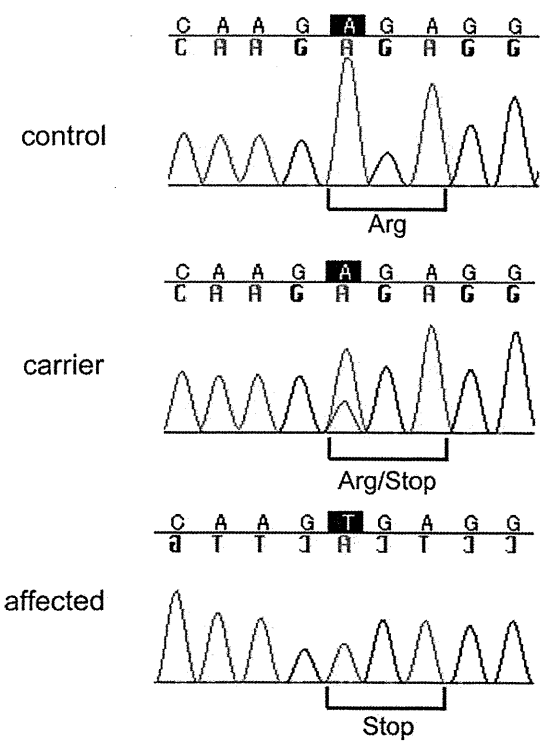

Figure 2 Electropherograms of a normal control, a carrier (mother) and the affected proband.

PMLD caused by *MCT8* mutations presents with infantile hypotonia, severe psychomotor development, nystagmus, generalised muscle weakness, dystopia, joint contracture and progressive spastic paraplegia. All affected male subjects develop the disease, while heterozygous female subjects are clinically normal or sometimes show mild thyroid dysfunction.[9 12] Brain MRI shows delayed myelination in the first few years of life, which subsequently improves but with residual neurological disability. The unique diagnostic feature of the disease is an abnormal thyroid hormone profile: increased free T_3, decreased free T_4 and normal thyroid-stimulating hormone.[12] The cases we analysed here showed clinical features and brain MRI findings typical of PMLD, but no thyroid hormone abnormalities. Based on regular laboratory testing and conventional PCR-based gene screening, we might have failed, or taken much longer, to identify the causative mutation. Thus, unbiased screening without prior knowledge is one of the advantages of NGS.

Thyroid hormone (T_4 and T_3) is important in neuronal development and its deficiency in the pre/neonatal stage causes a form of mental retardation called cretinism. T_4 is released from the thyroid as a prohormone and is altered to biologically active T_3 by iodothyronine deiodinases.[13] Active T_3 is delivered to the peripheral organs via thyroid hormone transporters. MCT8 is a thyroid hormone-specific transporter and is mainly expressed in the brain and liver.[14 15] In MCT8 deficiency, T_3 and T_4 uptake is impaired and deiodinase 2 is activated.[16] This results in increased serum T_3 levels because of T_3 accumulation in the peripheral blood. In previous reports, the majority of patients showed abnormal levels of thyroid hormones, but some displayed values within the normal range.[9 10 12 17 18] The variable range for abnormal thyroid hormone levels might be explained by unidentified modifier effect(s) and/or other transporter(s) that can compensate for MCT8 function.[19] Additionally, although MCT8 deficiency has been determined by abnormalities in thyroid function tests, it is unknown what proportion of the patients with MCT8 deficiency show abnormal thyroid function. We suggest that it is important to evaluate thyroid hormone function in PMLD with unknown cause.

Before the exome NGS analysis, we screened *PLP1*, *GJA12*, and seven other candidate genes mapped to the linked region: *MSN* (NM_002444), *IGBP1* (NM_001551), *SNX12* (NM_013346), *OGT* (NM_181672), *HDAC8* (NM_018486), *SH3BGRL* (NM_003022.2) and *PCDH11X* (NM_032967.2). Because we found no pathological changes, we adopted the exome sequencing strategy. We determined that exome sequencing with a single lane for each sample was sufficient to analyse all the transcripts of the X chromosome. In X-linked recessive diseases, male subjects are usually affected, and therefore the single X chromosome is the primary target of exome sequencing. Except for mosaic mutations, the hemizygous (rather than heterozygous) status of disease-related nucleotide changes is relatively easy to detect using all-or-none NGS reads (0% or 100% of reads). There was no difference in the ability of our two informatics methods (MAQ and NextGENe) to detect pathological changes. This approach could equally be applied to the analysis

of autosomal recessive diseases that manifest in the offspring of consanguineous relationships.

In conclusion, we rapidly identified a nonsense mutation in *MCT8* in a family with X-linked leucoencephalopathy using only a single lane of exome sequencing. This method is powerful for unbiased screening of disease-related mutations in X-linked or recessive conditions.

Acknowledgements We thank the family for their participation in this study.

Funding This work was supported by research grants from the Ministry of Health, Labour and Welfare (to HO, HSa, NMa and NMi), a grant-in-aid for scientific research from the Japan Society for the Promotion of Science (NMa), a grant-in-aid for young scientists from the Japan Society for the Promotion of Science (HSa), a grant from the 2010 Strategic Research Promotion of Yokohama City University (NMa), research grants from the Japan Epilepsy Research Foundation (HSa) and a research grant from the Naito Foundation (NMa). The study sponsors had no role in the study design; in the collection, analysis, and interpretation of the data; in the writing of the report; or in the decision to submit the paper for publication.

Competing interests None.

Patient consent Obtained.

Ethics approval This study was conducted with the approval of the institutional review board of Kanagawa Children's Medical Center and Yokohama City University School of Medicine.

Provenance and peer review Not commissioned; externally peer reviewed.

REFERENCES

1. **Shendure J,** Ji H. Next-generation DNA sequencing. *Nat Biotechnol* 2008;**26**:1135–45.
2. **Wheeler DA,** Srinivasan M, Egholm M, Shen Y, Chen L, McGuire A, He W, Chen YJ, Makhijani V, Roth GT, Gomes X, Tartaro K, Niazi F, Turcotte CL, Irzyk GP, Lupski JR, Chinault C, Song XZ, Liu Y, Yuan Y, Nazareth L, Qin X, Muzny DM, Margulies M, Weinstock GM, Gibbs RA, Rothberg JM. The complete genome of an individual by massively parallel DNA sequencing. *Nature* 2008;**452**:872–6.
3. **Ng SB,** Turner EH, Robertson PD, Flygare SD, Bigham AW, Lee C, Shaffer T, Wong M, Bhattacharjee A, Eichler EE, Bamshad M, Nickerson DA, Shendure J. Targeted capture and massively parallel sequencing of 12 human exomes. *Nature* 2009;**461**:272–6.
4. **Choi M,** Scholl UI, Ji W, Liu T, Tikhonova IR, Zumbo P, Nayir A, Bakkaloglu A, Ozen S, Sanjad S, Nelson-Williams C, Farhi A, Mane S, Lifton RP. Genetic diagnosis by whole exome capture and massively parallel DNA sequencing. *Proc Natl Acad Sci U S A* 2009;**106**:19096–101.
5. **Hodges E,** Xuan Z, Balija V, Kramer M, Molla MN, Smith SW, Middle CM, Rodesch MJ, Albert TJ, Hannon GJ, McCombie WR. Genome-wide in situ exon capture for selective resequencing. *Nat Genet* 2007;**39**:1522–7.
6. **Ng SB,** Buckingham KJ, Lee C, Bigham AW, Tabor HK, Dent KM, Huff CD, Shannon PT, Jabs EW, Nickerson DA, Shendure J, Bamshad MJ. Exome sequencing identifies the cause of a mendelian disorder. *Nat Genet* 2010;**42**:30–5.
7. **Nannya Y,** Sanada M, Nakazaki K, Hosoya N, Wang L, Hangaishi A, Kurokawa M, Chiba S, Bailey DK, Kennedy GC, Ogawa S. A robust algorithm for copy number detection using high-density oligonucleotide single nucleotide polymorphism genotyping arrays. *Cancer Res* 2005;**65**:6071–9.
8. **Li H,** Ruan J, Durbin R. Mapping short DNA sequencing reads and calling variants using mapping quality scores. *Genome Res* 2008;**18**:1851–8.
9. **Dumitrescu AM,** Liao XH, Best TB, Brockmann K, Refetoff S. A novel syndrome combining thyroid and neurological abnormalities is associated with mutations in a monocarboxylate transporter gene. *Am J Hum Genet* 2004;**74**:168–75.
10. **Friesema EC,** Grueters A, Biebermann H, Krude H, von Moers A, Reeser M, Barrett TG, Mancilla EE, Svensson J, Kester MH, Kuiper GG, Balkassmi S, Uitterlinden AG, Koehrle J, Rodien P, Halestrap AP, Visser TJ. Association between mutations in a thyroid hormone transporter and severe X-linked psychomotor retardation. *Lancet* 2004;**364**:1435–7.
11. **Frints SG,** Lenzner S, Bauters M, Jensen LR, Van Esch H, des Portes V, Moog U, Macville MV, van Roozendaal K, Schrander-Stumpel CT, Tzschach A, Marynen P, Fryns JP, Hamel B, van Bokhoven H, Chelly J, Beldjord C, Turner G, Gecz J, Moraine C, Raynaud M, Ropers HH, Froyen G, Kuss AW. *MCT8* mutation analysis and identification of the first female with Allan-Herndon-Dudley syndrome due to loss of *MCT8* expression. *Eur J Hum Genet* 2008;**16**:1029–37.
12. **Vaurs-Barriere C,** Deville M, Sarret C, Giraud G, Des Portes V, Prats-Vinas JM, De Michele G, Dan B, Brady AF, Boespflug-Tanguy O, Touraine R. Pelizaeus-Merzbacher-Like disease presentation of *MCT8* mutated male subjects. *Ann Neurol* 2009;**65**:114–18.
13. **Bianco AC,** Salvatore D, Gereben B, Berry MJ, Larsen PR. Biochemistry, cellular and molecular biology, and physiological roles of the iodothyronine selenodeiodinases. *Endocr Rev* 2002;**23**:38–89.
14. **Friesema EC,** Ganguly S, Abdalla A, Manning Fox J, Halestrap AP, Visser TJ. Identification of monocarboxylate transporter 8 as a specific thyroid hormone transporter. *J Biol Chem* 2003;**41**:40128–35.
15. **Lafreniere RG,** Carrel L, Willard HF. A novel transmembrane transporter encoded by the XPCT gene in Xq13.2. *Hum Mol Genet* 1994;**3**:1133–9.
16. **Dumitrescu AM,** Liao XH, Weiss RE, Millen K, Refetoff S. Tissue-specific thyroid hormone deprivation and excess in monocarboxylate transporter (mct) 8-deficient mice. *Endocrinology* 2006;**147**:4036–43.
17. **Maranduba CM,** Friesema EC, Kok F, Kester MH, Jansen J, Sertie AL, Passos-Bueno MR, Visser TJ. Decreased cellular uptake and metabolism in Allan-Herndon-Dudley syndrome (AHDS) due to a novel mutation in the MCT8 thyroid hormone transporter. *J Med Genet* 2006;**43**:457–60.
18. **Namba N,** Etani Y, Kitaoka T, Nakamoto Y, Nakacho M, Bessho K, Miyoshi Y, Mushiake S, Mohri I, Arai H, Taniike M, Ozono K. Clinical phenotype and endocrinological investigations in a patient with a mutation in the MCT8 thyroid hormone transporter. *Eur J Pediatr* 2008;**167**:785–91.
19. **Herzovich V,** Vaiani E, Marino R, Dratler G, Lazzati JM, Tilitzky S, Ramirez P, Iorcansky S, Rivarola MA, Belgorosky A. Unexpected peripheral markers of thyroid function in a patient with a novel mutation of the MCT8 thyroid hormone transporter gene. *Horm Res* 2007;**67**:1–6.

CLINICAL GENETICS An International Journal of Genetics, Molecular and Personalized Medicine

Clin Genet 2011: 80: 161–166
Printed in Singapore. All rights reserved

CLINICAL GENETICS
doi: 10.1111/j.1399-0004.2011.01721.x

Short Report

Exome sequencing of two patients in a family with atypical X-linked leukodystrophy

Tsurusaki Y, Okamoto N, Suzuki Y, Doi H, Saitsu H, Miyake N, Matsumoto N. Exome sequencing of two patients in a family with atypical X-linked leukodystrophy.
Clin Genet 2011: 80: 161–166. © John Wiley & Sons A/S, 2011

We encountered a family with two boys similarly showing brain atrophy with reduced white matter, hypoplasia of the brain stem and corpus callosum, spastic paralysis, and severe growth and mental retardation without speaking a word. The phenotype of these patients was not compatible with any known type of syndromic leukodystrophy. Presuming an X-linked disorder, we performed next-generation sequencing (NGS) of the transcripts of the entire X chromosome. A single lane of exome NGS in each patient was sufficient. Six potential mutations were found in both affected boys. Two missense mutations, including c.92T>C (p.V31A) in *L1CAM*, were potentially pathogenic, but this remained inconclusive. The other four could be excluded. Because the patients did not show adducted thumbs or hydrocephalus, the *L1CAM* change in this family can be interpreted as different scenarios. Personal genome analysis using NGS is certainly powerful, but interpretation of the data can be a substantial challenge requiring a lot of tasks.

Conflict of interest

None of the authors have any conflicts of interest to disclose.

Y Tsurusaki[a], N Okamoto[b], Y Suzuki[c], H Doi[a], H Saitsu[a], N Miyake[a] and N Matsumoto[a]

[a]Department of Human Genetics, Yokohama City University Graduate School of Medicine, Kanazawa-ku, Yokohama, Japan, and [b]Department of Medical Genetics, and [c]Department of Pediatric Neurology, Osaka Medical Center and Research Institute for Maternal and Child Health, Murodo-cho, Izumi, Japan

Key words: atypical phenotype – exome sequencing – *L1CAM* – X-linked leukodystrophy

Corresponding author: Naomichi Matsumoto, Department of Human Genetics, Yokohama City University Graduate School of Medicine, 3-9 Fukuura, Kanazawa-ku, Yokohama 236-0004, Japan.
Tel.: +81-45-787-2606;
fax: +81-45-786-5219;
e-mail: naomat@yokohama-cu.ac.jp

Received 4 May 2011, revised and accepted for publication 31 May 2011

Focused/selected gene and genomic characterization has usually been carried out in clinically homogeneous groups of multiple affected samples to make identification of genetic abnormalities more efficient. Microarrays and next-generation sequencing (NGS) have provided new avenues for human genetic research (1–6). Using such new technologies, researchers are able to analyze small numbers of patients on a genome-wide scale. Even very rare cases (such as when only a few compatible patients are available or atypical patients showing no similar phenotypes) can be realistic targets of genetic research, as the new technologies can identify aberrations in a single gene from within virtually the whole genome; this could not be achieved with conventional techniques.

We encountered a family with two affected males showing atypical leukodystrophy. The phenotype of these patients did not match any known type of syndromic leukodystrophy. Because we presumed that abnormality of an X-linked gene caused the atypical leukodystrophy in this family, we performed exome sequencing of most of the X-chromosome transcripts and identified an unexpected gene mutation in these patients.

Materials and methods

A family with atypical X-linked leukodystrophy

Two brothers, II-1 currently aged 19 years and II-2 currently aged 17 years, who have unrelated healthy parents, presented with similar clinical

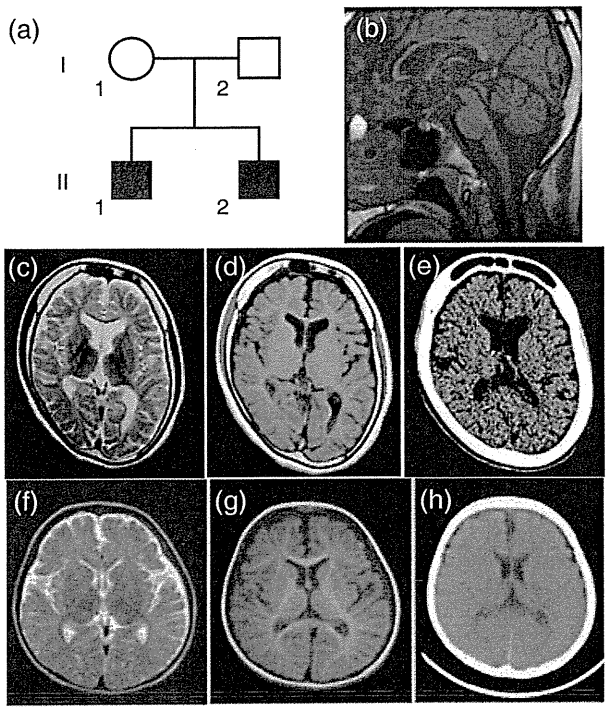

Fig. 1. Clinical features of the family. Familial pedigree (**a**). Brain magnetic resonance imaging (MRI) (**b**: T1-weighted image, **c**: T2-weighted image, **d**: T1-weighted image) of individual II-1 at 16 years old showing hypoplasia of the white matter, the brain stem and the corpus callosum. Brain computed tomographic (CT) images of individual II-1 at 19 years old (**e**) indicating a thick calvarium with enlarged frontal sinus as well as calcification of the choroid plexus in the atrophic brain. Brain MRI (**f**: T2-weighted image, **g**: T1-weighted image) of individual II-2 at 2 years old, also displaying hypoplasia of the white matter. Brain CT image of individual II-2 at 5 years old (**h**), also showing a thick calvarium.

features. Their mother did not show any neurological abnormalities (Fig. 1a).

Patient II-1

Patient II-1's birth weight was 2840 g at 40 weeks of gestational age. He had congenital nystagmus. He sat unsupported at 7 months old but after this his developmental milestones were delayed. He could creep at 18 months old. Spastic paralysis, especially in the lower extremities, became apparent. He was unable to stand unsupported. His mental development was severely delayed, and he needed special education from elementary school. He had suffered generalized epileptic seizures since he was 10 years old. He was confined to a wheelchair. He had severe mental retardation without speaking a word. His developmental quotient (DQ) at 9 years old was 19 by the Japanese standard method. Severe growth retardation [143 cm (<3%), 24 kg (<3%), occipitofrontal head circumference 49 cm (<3%) at 19 years] was also noted. He did not have dysmorphic features. Blood analysis revealed microcytic anemia [hemoglobin (Hb) 13.4 g/dl, mean corpuscular volume (MCV) (of red blood cell) 70.4 fl (normal: 89–99 fl), mean corpuscular hemoglobin (MCH) (of red blood cell) 23.1 pg (normal: 29–35 pg)] without any evidence of hemolysis or iron deficiency. Hormonal examination indicated that the levels of luteinizing hormone, follicle-stimulating hormone, and thyroid-stimulating hormone were all low [0.9 mIU/ml (normal: 1.2–8.0 mIU/ml), 2.5 mIU/ml (normal: 2.3–15.1 mIU/ml), <0.01 μIU/ml (normal: 0.5–5.0 μIU/ml), respectively]. He showed delayed puberty with small testes. Pubic hair only appeared at 17 years old. His bone age at 18 years old was 12.6 years (67%). Brain magnetic resonance imaging (MRI) at 16 years old revealed brain atrophy associated with reduced white matter and hypoplasia of the brain stem and the corpus callosum (Fig. 1b–d). No hydrocephalus or adducted thumb was observed. Brain computed tomography (CT) at 19 years old showed a thick calvarium with enlarged frontal sinus as well as calcification of the cerebellar tentorium and the choroid plexus (Fig. 1e).

Patient II-2

Patient II-2's birth weight was 2910 g at 37 weeks of gestational age. Developmental delay was apparent since he was 10 months old. Spastic paralysis (especially in the lower extremities), confinement to a wheelchair, severe mental retardation without speaking a word (DQ = 5 at 17 years old), and severe growth retardation [130 cm (<3%) and 27 kg (<3%) at 17 years] were phenotypes shared with his brother (II-1). Blood analysis revealed microcytic anemia (Hb 12.0 g/dl, MCV 61.1 fl, MCH 19.0 pg) without any evidence of hemolysis or iron deficiency. Hormonal examination indicated that the levels of luteinizing hormone, follicle-stimulating hormone, and thyroid-stimulating hormone were relatively low (1.9 mIU/ml, 4.2 mIU/ml, <0.23 μIU/ml, respectively). He also showed delayed puberty with small testes. Pubic hair appeared only at 17 years old. His bone age at 17 years old was 11 years (65%). Brain MRI at 2 years old revealed brain atrophy associated with reduced white matter and hypoplasia of the brain stem and corpus callosum (Fig. 1f,g). Brain CT at 5 years old showed a thick calvarium (Fig. 1h). No hydrocephalus or adducted thumb was observed. Most of the clinical features were similar to those of his brother except for the absence of nystagmus in patient II-2.

Genome-wide SNP genotyping

Genome-wide single-nucleotide polymorphism (SNP) genotyping was performed on individuals I-2, II-1, and II-2 using a GeneChip™ Human Mapping 10K Array Xba 142 2.0 (Affymetrix, Inc., Santa Clara, CA), according to the manufacturer's protocols. Mendelian error in the pedigree to exclude conflicted SNPs was checked using GCOS 1.2 (GeneChip Operating Software; Affymetrix) and batch analysis in GTYPE 4.0 (GeneChip Genotyping Analysis Software; Affymetrix), with the default setting for the mapping algorithm. The linked region, with SNP genotypes shared between individuals II-1 and II-2, was checked manually.

Genomic partitioning, short-read sequencing, and sequence alignment

Three micrograms of genomic DNA from the affected brothers (II-1 and II-2) was processed using a SureSelect X Chromosome test kit (1582 transcripts covering 3053 kb) (Agilent Technologies, Santa Clara, CA), according to the manufacturer's instructions. Captured DNAs were analyzed using an Illumina GAIIx (Illumina, Inc., San Diego, CA). We used only one of the eight lanes in the flow cell (Illumina) for paired-end, 76-bp reads per sample. Image analysis and base-calling were performed using sequence control software (SCS) real-time analysis and off-line BASECALLER software v1.8.0 (Illumina). Reads were aligned to the human reference genome (UCSC hg19, NCBI build 37.1) using the ELANDv2 algorithm in CASAVA_v1.7.0 (Illumina). The ELANDv2 algorithm can align 100-bp reads to a reference sequence and split the reads into multiple seeds.

Mapping strategy and variant annotation

Approximately 57.5 million reads from individual II-1 and 71.1 million reads from individual II-2 that passed the quality control (Path Filter) were mapped to the human reference genome using mapping and assembly with quality (MAQ) (7) (Fig. 2). MAQ was able to align 51 720 952 and 65 990 660 reads to the whole genome for individuals II-1 and II-2, respectively; these were then statistically analyzed for coverage using a script created by BITS Co., Ltd. (Tokyo, Japan). SNPs and insertions/deletions were extracted from the alignment data using an original script created by BITS Co., Ltd., along with information on the registered SNPs (dbSNP 131). A consensus quality score of 40 or more was used for the SNP analysis in MAQ. SNPs in MAQ-passed reads were annotated using the SeattleSeq website (http://gvs.gs.washington.edu/SeattleSeqAnnotation/). Variants found by each informatics method were selected in terms of location on chromosome X, unregistered variants (excluding registered SNPs), variants in known genes, variants in coding regions, variants excluding synonymous changes, and variants with an allele frequency of at least 90% (assuming a homozygous mutation). NEXTGENE software v2.0 (SoftGenetics, State College, PA) was also used to analyze the reads, with a default setting. Variants found by both of the informatics methods were selected. The variants found in common between individuals II-1 and II-2 were focused on, and confirmed as true positives by Sanger sequencing of polymerase chain reaction (PCR) products amplified from patient genomic DNA, except for variants within genes at segmental duplications. The pathological significance of the variants was evaluated using four different websites: POLYPHEN (Polymorphism Phenotyping; http://genetics.bwh.harvard.edu/pph/index.html), POLYPHEN-2 (http://genetics.bwh.harvard.edu/pph2/index.shtml), SIFT (http://sift.jcvi.org/) (output values less than 0.05 are deleterious), and MUTATIONTASTER (http://neurocore.charite.de/MutationTaster/).

Capillary sequencing

Possible pathological variants were confirmed by Sanger sequencing using an ABI 3500xl or ABI3100 autosequencer (Life Technologies, Carlsbad, CA), following the manufacturer's protocol. Sequencing data were analyzed using SEQUENCHER software (Gene Codes Corporation, Ann Arbor, MI).

Expression studies

The relative mRNA levels of *TMEM187* in cDNA of various fetal and adult human tissues (Human MTC™ Panel I and Human Fetal MTC™ Panel; Clontech, Mountain View, CA) were determined by quantitative real-time reverse transcription–polymerase chain reaction (RT-PCR) using TaqMan gene expression assays (Hs01920894_s1 for *TMEM187* and Hs00357333_g1 for β-actin as a control) (Life Technologies).

Results and discussion

Our coverage analysis indicated that for individuals II-1 and II-2, 79.2% and 78.8%, respectively, of the entire X-chromosome coding sequence (CDS) were completely covered, and 88.5% and 88.5%,

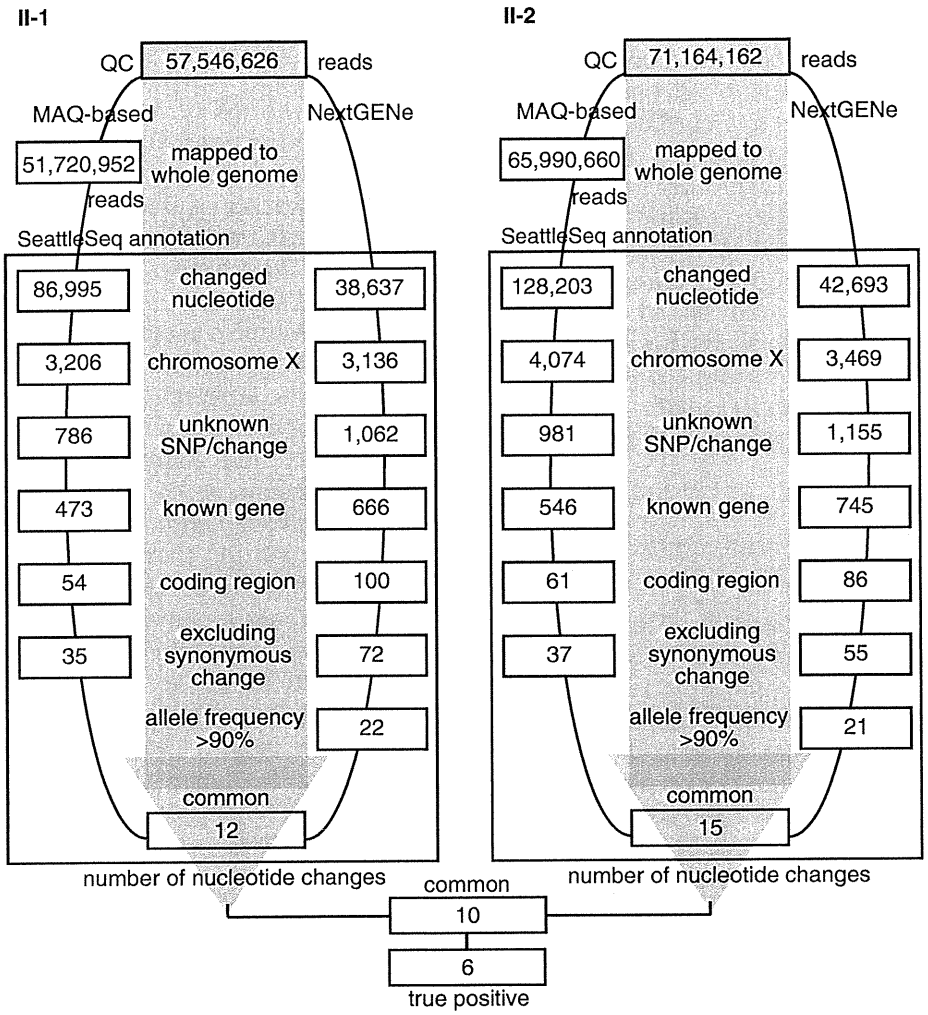

Fig. 2. Flow of informatics analysis. A MAQ-based method and NextGENe analysis were performed in individuals II-1 and II-2. The selection methods employed included variants compared with the human genome reference sequence, variants mapped to chromosome X, unknown variants [excluding registered single-nucleotide polymorphisms (SNPs)], variants in known genes, variants in coding regions, variants excluding synonymous changes, and variants common to the two informatics methods. Finally, the nucleotide changes in common between individuals II-1 and II-2 were focused on as potentially pathogenic mutations. True positive changes were confirmed by capillary sequencing of polymerase chain reaction (PCR) products amplified from genomic DNA.

respectively, of the CDS were at least 90% covered by reads. Using a single lane of sequencing per sample, the coverage with 20 reads or more comprised 89.6% and 89.7% of the CDS, and that with 100 reads or more comprised 87.6% and 89.7% of the CDS in individuals II-1 and II-2, respectively. SNP genotyping indicated that the region from rs727240 to rs721003 (UCSC genome browser hg19 assembly, chromosome X coordinates: 22131639–54454152; 32.2 Mb) was unlinked to the phenotype. Exome sequencing using two informatics methods successfully identified six potentially interesting changes as true positives in the linked region: *FAM123B* (RefSeq Gene ID NM_152424): c.85G>A (p.A29T), *FRMD7* (NM_194277): c.875T>C (p.L292P), *L1CAM* (NM_000425): c.92T>C (p.V31A), *TMEM187* (NM_003492): c.334G>A (p.A112T), *FLNA* (NM_001110556): c.1582G>A (p.V528M), and *LAGE3* (NM_006014): c.395G>A (p.R132Q).

The c.92T>C (p.V31A) variant in *L1CAM* was previously found in a patient with Hirschsprung disease, acrocallosal syndrome, and congenital hydrocephalus (8). *L1CAM* mutations cause a wide variety of clinical phenotypes: hydrocephalus due to stenosis of the aqueduct of Sylvius (MIM #307000), MASA syndrome (mental retardation, aphasia, shuffling gait, adducted thumb; MIM #303350), and X-linked agenesis of the corpus callosum (MIM #217990). Phenotypic variability, even within a family, has been noted, raising the caution that definite clinical diagnosis in single

Table 1. Characterization of nucleotide changes found by exome sequencing

	FAM123B	*FRMD7*	*L1CAM*	*TMEM187*	*FLNA*	*LAGE3*
Change	c.85G>A (p.A29T)	c.875T>C (p.L292P)	c.92T>C (p.V31A)	c.334G>A (p.A112T)	c.1582G>A (p.V528M)	c.395G>A (p.R132Q)
PolyPhen	Benign	Probably damaging	Benign	Benign	Possibly damaging	Benign
PolyPhen-2	Probably damaging	Probably damaging	Benign	Possibly damaging	Possibly damaging	Possibly damaging
SIFT	0.04	0.02	0.22	0.02	0.04	0.46
MutationTaster	Polymorphism	Disease causing	Disease causing	Polymorphism	Polymorphism	Polymorphism
Normal female	8/502[a]	2/502	2/502	1/502	15/502[a]	4/502
Normal male	1/118	0/117	0/118	0/118		1/86
Note		No nystagmus in II-2				

[a]Including one homozygous female. Underlining means that this result excludes the variant as potentially causative. Grayed shading indicates the variants that could not be excluded; between these two, the *L1CAM* variant is more likely to be causative.

cases is often impossible (9). Phenotypic features compatible with the *L1CAM* mutation in our patients include spastic paralysis, aphasia, severe mental and growth retardation, but atypical leukodystrophy and the absence of adducted thumbs were very rare or exceptional (9). A normal control study found that 2 of 251 normal females were heterozygous for this SNP, but none of 117 normal males carried the variant allele. One of the four web-based analyses of pathological significance (MutationTaster) indicated that this variant would be disease causing, while the others indicated that it would be benign (Table 1). X-linked hydrocephalus due to *L1CAM* mutations occurs in approximately 1/30 000 male births (10). Considering that the *L1CAM* mutation was found in 2/618 control alleles (0.32%), the change may be a rare polymorphism, a mutation causing lethality in the majority of affected males, or a mutation with low penetrance. Because we were unable to exclude this *L1CAM* change, its pathogenic status remains inconclusive.

We next examined c.85G>A in *FAM123B*, c.875T>C in *FRMD7*, c.1582G>A in *FLNA*, and c.395G>A in *LAGE3* in normal controls. The *FAM123B*, *FLNA*, and *LAGE3* variants were excluded as causative because a homozygous change was found in 1 of 251 female controls (*FAM123B* and *FLNA*) or a hemizygous change was found in 1 of 86 normal males (*LAGE3*). However, the thick calvarium in individuals II-1 and II-2 may be influenced by the *FAM123B* change, because it is causative for osteopathia striata with cranial sclerosis, an X-linked dominant disorder (MIM #300373) (11, 12). As the calvarium of the patients' mother having the heterozygous *FAM123B* change was not evaluated by CT, we could not confirm this possibility.

Only 2 of 251 control females carried the c.875T>C variant in *FRMD7* heterozygously, and none of 117 male controls carried this variant; thus, the pathogenicity of the *FMRD7* variant was inconclusive. Other *FRMD7* mutations cause X-linked congenital nystagmus 1 (MIM #310700) (13). However, the nystagmus found in individual II-1 was not observed in individual II-2, indicating that the variant in common between two brothers did not consistently cause nystagmus. Thus, it may not contribute to the phenotype in this family (Table 1).

We also evaluated the c.334G>A variant in *TMEM187*. Only 2 of 251 female controls carried this heterozygous change, and it was not found among 118 male controls. Two of the four programs (PolyPhen-2 and SIFT) indicated that it would be pathogenic. By Taqman assay, *TMEM187* was ubiquitously expressed in various fetal and adult tissues, including the brain (data not shown), leaving the effect of this mutation on the phenotype in these patients inconclusive (Table 1).

In conclusion, we found two possible but inconclusive variants in this family with two boys affected by atypical leukodystrophy. High-throughput technologies are clearly powerful to detect genomic changes, but evaluation of the data can be very difficult and should be performed cautiously. More knowledge of rare SNPs and mutations is absolutely necessary before any conclusions can be drawn.

Acknowledgements

We would like to thank the patients and their family members for their participation in this study. This work was supported by research grants from the Ministry of Health, Labour and Welfare

(to H. S., N. Miyake, and N. Matsumoto), the Japan Science and Technology Agency (to N. Matsumoto), a Grant-in-Aid for Scientific Research from the Japan Society for the Promotion of Science (to N. Matsumoto), and a Grant-in-Aid for Young Scientists from the Japan Society for the Promotion of Science (to H. D., N. Miyake, and H. S.).

References

1. Saitsu H, Kato M, Mizuguchi T et al. De novo mutations in the gene encoding STXBP1 (MUNC18-1) cause early infantile epileptic encephalopathy. Nat Genet 2008: 40: 782–788.
2. Check Hayden E. Genomics shifts focus to rare diseases. Nature 2009: 461: 458.
3. Biesecker LG. Exome sequencing makes medical genomics a reality. Nat Genet 2010: 42: 13–14.
4. Kuhlenbaumer G, Hullmann J, Appenzeller S. Novel genomic techniques open new avenues in the analysis of monogenic disorders. Hum Mutat 2011: 32: 144–151.
5. Miyake N, Kosho T, Mizumoto S et al. Loss-of-function mutations of CHST14 in a new type of Ehlers-Danlos syndrome. Hum Mutat 2010: 31: 966–974.
6. Ng SB, Bigham AW, Buckingham KJ et al. Exome sequencing identifies MLL2 mutations as a cause of Kabuki syndrome. Nat Genet 2010: 42: 790–793.
7. Li H, Ruan J, Durbin R. Mapping short DNA sequencing reads and calling variants using mapping quality scores. Genome Res 2008: 18: 1851–1858.
8. Nakakimura S, Sasaki F, Okada T et al. Hirschsprung's disease, acrocallosal syndrome, and congenital hydrocephalus: report of 2 patients and literature review. J Pediatr Surg 2008: 43: E13–E17.
9. Rietschel M, Friedl W, Uhlhaas S, Neugebauer M, Heimann D, Zerres K. MASA syndrome: clinical variability and linkage analysis. Am J Med Genet 1991: 41: 10–14.
10. Rosenthal A, Jouet M, Kenwrick S. Aberrant splicing of neural cell adhesion molecule L1 mRNA in a family with X-linked hydrocephalus. Nat Genet 1992: 2: 107–112.
11. Viot G, Lacombe D, David A et al. Osteopathia striata cranial sclerosis: non-random X-inactivation suggestive of X-linked dominant inheritance. Am J Med Genet 2002: 107: 1–4.
12. Jenkins ZA, van Kogelenberg M, Morgan T et al. Germline mutations in WTX cause a sclerosing skeletal dysplasia but do not predispose to tumorigenesis. Nat Genet 2009: 41: 95–100.
13. Tarpey P, Thomas S, Sarvananthan N et al. Mutations in FRMD7, a newly identified member of the FERM family, cause X-linked idiopathic congenital nystagmus. Nat Genet 2006: 38: 1242–1244.

REPORT

Mutations in *POLR3A* and *POLR3B* Encoding RNA Polymerase III Subunits Cause an Autosomal-Recessive Hypomyelinating Leukoencephalopathy

Hirotomo Saitsu,[1,*] Hitoshi Osaka,[2] Masayuki Sasaki,[3] Jun-ichi Takanashi,[4] Keisuke Hamada,[5] Akio Yamashita,[6] Hidehiro Shibayama,[7] Masaaki Shiina,[5] Yukiko Kondo,[1] Kiyomi Nishiyama,[1] Yoshinori Tsurusaki,[1] Noriko Miyake,[1] Hiroshi Doi,[1] Kazuhiro Ogata,[5] Ken Inoue,[8] and Naomichi Matsumoto[1,*]

Congenital hypomyelinating disorders are a heterogeneous group of inherited leukoencephalopathies characterized by abnormal myelin formation. We have recently reported a hypomyelinating syndrome characterized by diffuse cerebral hypomyelination with cerebellar atrophy and hypoplasia of the corpus callosum (HCAHC). We performed whole-exome sequencing of three unrelated individuals with HCAHC and identified compound heterozygous mutations in *POLR3B* in two individuals. The mutations include a nonsense mutation, a splice-site mutation, and two missense mutations at evolutionally conserved amino acids. Using reverse transcription-PCR and sequencing, we demonstrated that the splice-site mutation caused deletion of exon 18 from *POLR3B* mRNA and that the transcript harboring the nonsense mutation underwent nonsense-mediated mRNA decay. We also identified compound heterozygous missense mutations in *POLR3A* in the remaining individual. *POLR3A* and *POLR3B* encode the largest and second largest subunits of RNA Polymerase III (Pol III), RPC1 and RPC2, respectively. RPC1 and RPC2 together form the active center of the polymerase and contribute to the catalytic activity of the polymerase. Pol III is involved in the transcription of small noncoding RNAs, such as 5S ribosomal RNA and all transfer RNAs (tRNA). We hypothesize that perturbation of Pol III target transcription, especially of tRNAs, could be a common pathological mechanism underlying *POLR3A* and *POLR3B* mutations.

Congenital hypomyelinating disorders form a heterogeneous group of central nervous system leukoencephalopathies that is characterized by abnormal myelin formation. Although these conditions are readily recognized by brain magnetic resonance imaging (MRI), many cases are not diagnosed correctly.[1] Several syndromes affecting myelination, such as hypomyelination with hypodontia and hypogonadotropic hypogonadism (4H) syndrome (MIM 612440) and hypomyelination with atrophy of the basal ganglia and cerebellum (H-ABC) (MIM 612438), have been described.[2–5] We have recently reported a hypomyelinating syndrome characterized by diffuse cerebral hypomyelination with cerebellar atrophy and hypoplasia of the corpus callosum (HCAHC).[6] Individuals with HCAHC do not show hypodontia or atrophy of the basal ganglia, which are observed in 4H syndrome and H-ABC; however, diffuse hypomyelination, atrophy, or hypoplasia of the cerebellum and corpus callosum are overlapping features of these three syndromes, suggesting that there might be a common underlying pathological mechanism.

Here, we report on four individuals with HCAHC from three unrelated families (Figure 1A; Table 1). Clinical information and peripheral blood or saliva samples were obtained from the family members after obtaining written informed consent. Experimental protocols were approved by the Institutional Review Board of Yokohama City University. To identify pathogenic mutations, we performed whole-exome sequencing of three probands from three unrelated families (individuals 1, 3, and 4). DNAs were captured with the SureSelect Human All Exon 50Mb Kit (Agilent Technologies, Santa Clara, CA) and sequenced with one lane per sample on an Illumina GAIIx (Illumina, San Diego, CA) with 108 bp paired-end reads. Image analysis and base calling were performed by sequence control software real-time analysis and CASAVA software v1.7 (Illumina). A total of 90,014,368 (individual 1), 86,942,264 (individual 3), and 92,168,758 (individual 4) paired-end reads were obtained and aligned to the human reference genome sequence (GRCh37/hg19) with MAQ[7] and NextGENe software v2.00 with sequence condensation by consolidation (SoftGenetics, State College, PA). This approach resulted in more than 88% of target exomes being covered by ten reads or more (see Table S1, available online). Single nucleotide variants (SNVs) were called with MAQ and NextGENe. Small insertions and deletions were

[1]Department of Human Genetics, Yokohama City University Graduate School of Medicine, 3-9 Fukuura, Kanazawa-ku, Yokohama 236-0004, Japan; [2]Division of Neurology, Clinical Research Institute, Kanagawa Children's Medical Center, 2-138-4 Mutsukawa, Minami-ku, Yokohama 232-8555, Japan; [3]Department of Child Neurology, National Center of Neurology and Psychiatry, 4-1-1 Ogawahigashi-cho Kodaira, Tokyo 187-8551, Japan; [4]Department of Pediatrics, Kameda Medical Center, 929 Higashi-cho, Kamogawa-shi, Chiba 296-8602, Japan; [5]Department of Biochemistry, Yokohama City University Graduate School of Medicine, 3-9 Fukuura, Kanazawa-ku, Yokohama 236-0004, Japan; [6]Department of Molecular Biology, Yokohama City University Graduate School of Medicine, 3-9 Fukuura, Kanazawa-ku, Yokohama 236-0004, Japan; [7]Department of Neurology, Kameda Medical Center, 929 Higashi-cho, Kamogawa-shi, Chiba 296-8602, Japan; [8]Department of Mental Retardation and Birth Defect Research, National Institute of Neuroscience, National Center of Neurology and Psychiatry, 4-1-1 Ogawahigashi-cho Kodaira, Tokyo 187-8551, Japan
*Correspondence: hsaitsu@yokohama-cu.ac.jp (H.S.), naomat@yokohama-cu.ac.jp (N.M.)
DOI 10.1016/j.ajhg.2011.10.003.

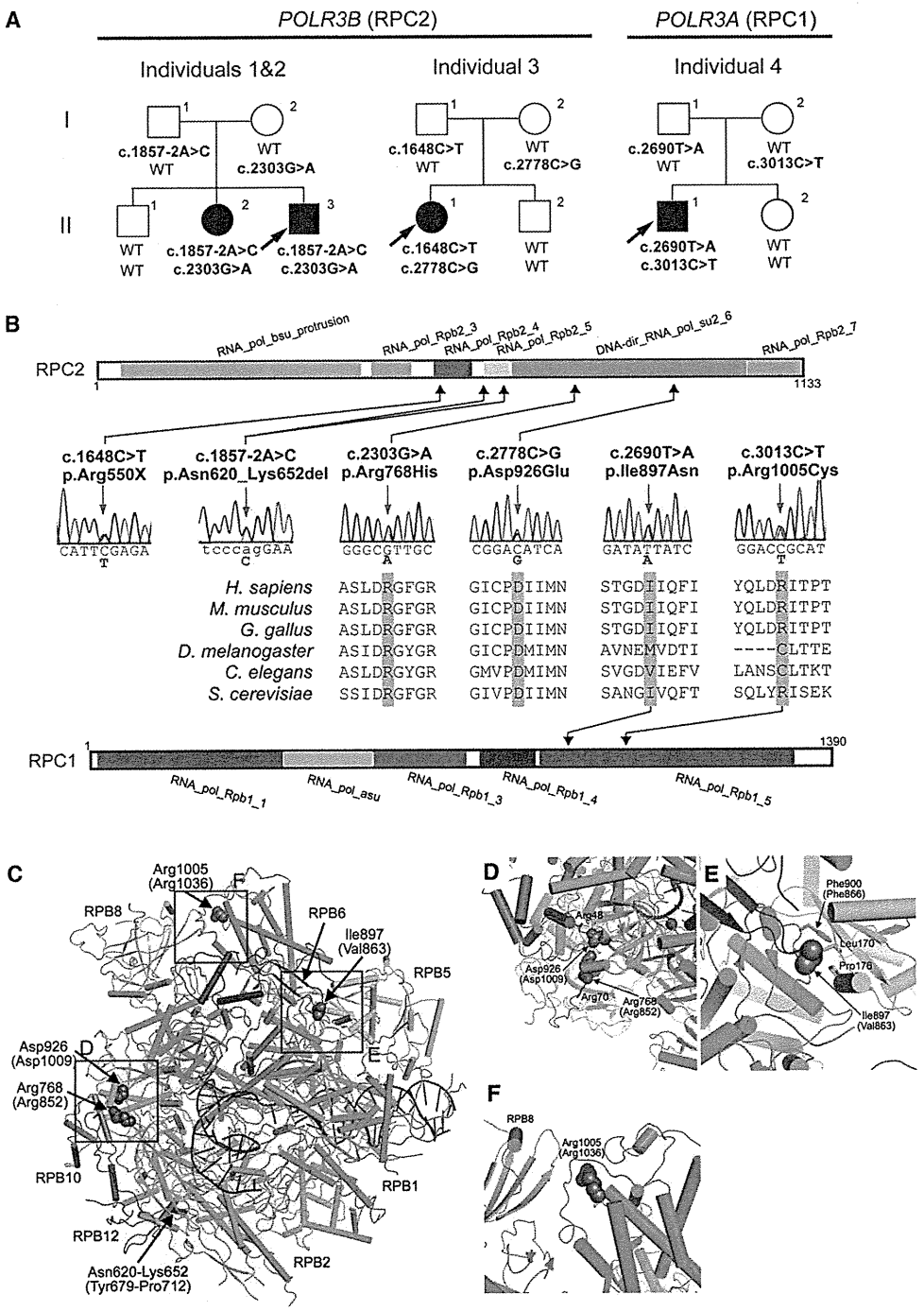

Figure 1. Mutations in *POLR3B* and *POLR3A*

(A) Pedigrees of four kindreds with HCAHC are shown. We identified four mutations in *POLR3B* encoding RPC2 in three individuals from two unrelated families and two mutations in *POLR3A* encoding RPC1 in one family. The segregation of each mutation is shown.

(B) Schematic representation of RPC2 (upper) and RPC1 (lower) proteins with Pfam domains (from Ensembl). Locations of each amino-acid-altering mutation are depicted with electropherograms. All of the missense mutations occurred at evolutionally conserved amino acids. Homologous sequences were aligned with the CLUSTALW website.

(C–F) 3D representations of RPC1 and RPC2 mutations. Mutated amino acids in RPC1 and RPC2 are shown along with their equivalent positions in the homologous RPB1 and RPB2 subunits of RNA Polymerase II (amino acid and its position in parenthesis). The structure and positions of mutations are illustrated by PyMOL with the crystal structure (PDB accession number 3GTP). RPB3, RPB9, and RPB11 subunits, which are specific to RNA Polymerase II, have been omitted from the figure. RPB1 is shown in green, RPB2 in sky blue, RPB5 in yellow, RPB6 in dark blue, RPB8 in pink, RPB10 in orange, RPB12 in purple, DNA in brown, and RNA in red. Amino acids that interact with mutated amino acids are also shown.

Table 1. Clinical Features of the Individuals

Clinical Features	Individual 1	Individual 2	Individual 3	Individual 4
Genes	*POLR3B*	*POLR3B*	*POLR3B*	*POLR3A*
Mutations, DNA	c.1857-2A>C, c.2303G>A	c.1857-2A>C, c.2303G>A	c.1648C>T, c.2778C>G	c.2690T>A, c.3013C>T
Mutations, protein	p.Asn620_Lys652del, p.Arg768His	p.Asn620_Lys652del, p.Arg768His	p.Arg550X, p.Asp926Glu	p.Ile897Asn, p.Arg1005Cys
Gender	M	F	F	M
Current age (years)	27	30	16	17
Intellectual disability	mild	mild	moderate	mild
Cognitive regression	–	–	–	–
Seizures	–	–	–	–
Initial motor development	normal	normal	normal	normal
Age of onset (years)	3	3	2	4
Motor deterioration	–	–	–	+
Wheelchair use	–	–	–	+
Optic atrophy	–	–	–	–
Myopia	+	+	–	+
Nystagmus	+	+	–	–
Abnormal pursuit	+	+	+	–
Vertical gaze limitation	+	+	+	–
Dysphagia	–	–	+	–
Hypersalivation	–	–	–	–
Cerebellar signs	+	+	+	+
Tremor	–	+	+	+
Babinski refex	–	–	–	–
Spasticity	–	–	mild	–
Peripheral nerve involvement	–	–	–	–
Nerve biopsy	NA	NA	NA	NA
Hypodontia	–	–	–	–
Hypogonadism	+	+	–	–

NA is an abbreviation for not available.

detected with NextGENe. Called SNVs were annotated with SeattleSeq Annotation.

We adopted a prioritization scheme to identify the pathogenic mutation in each individual, similar to the approach taken by recent studies (Table S2).[8–10] First, we excluded the variants registered in the dbSNP131 or 1000 Genome Project from all the detected variants. Then, SNVs commonly detected by MAQ and NextGENe analyses were selected as highly confident variants; 364 to 374 SNVs of nonsynonymous (NS) or canonical splice-site (SP) changes, along with 113 to 124 small insertions or deletions (indels), were identified per individual. We also excluded variants found in our 55 in-house exomes, which are derived from 12 healthy individuals and 43 individuals with unrelated diseases, reducing the number of candidate variants to ~250 per individual. Assuming that HCAHC is an autosomal-recessive disorder based on two affected individuals in one pedigree (individuals 1 and 2), we focused on rare heterozygous variants that are not registered in the dbSNP or in our in-house 55 exomes.

We surveyed all genes in each individual for two or more NS, SP, or indel variants. We found three to eight candidate genes per individual (Table S2). Among them, only *POLR3B* encoding RPC2, the second largest subunit of RNA Polymerase III (Pol III), was common in two individuals (individuals 1 and 3). The inheritance of the variants in *POLR3B* (transcript variant 1, NM_018082.5) was examined by Sanger sequencing. In individual 1, we confirmed that a canonical splice-site mutation (c.1857-2A>C [p.Asn620_Lys652del]), 2 bp upstream of exon 18, was

inherited from his father, and that a missense mutation (c.2303G>A [p.Arg768His]) in exon 21 were inherited from his mother (Figure 1A). The two mutations were also present in an affected elder sister (individual 2) but not present in a healthy elder brother. In individual 3, we confirmed that a nonsense mutation (c.1648C>T [p.Arg550X]) in exon 16 was inherited from her father and that a missense mutation (c.2778C>G [p.Asp926Glu]) in exon 24 was inherited from her mother (Figure 1A). The two mutations were not present in a healthy younger brother. To examine the mutational effects of c.1857-2A>C and c.1648C>T, reverse transcription PCR and sequencing with total RNA extracted from lymphoblastoid cells derived from the individuals was performed as previously described.[11] We demonstrated that the c.1857-2A>C mutation caused deletion of exon 18 from the *POLR3B* mRNA (Figures 2A–2C), resulting in an in-frame 33 amino acid deletion (p.Asn620_Lys652del) from RPC2 (Figure 1B). In addition, the mutated transcript harboring the nonsense mutation (c.1648C>T) was found to be expressed at a much lower level compared with the wild-type transcript (Figure 2D). The expression level of the mutated transcript was increased after treatment with 30 μM cycloheximide (CHX),[11] which inhibits nonsense-mediated mRNA decay (NMD), indicating that the mutant transcript underwent NMD (Figure 2D). The two missense mutations (p.Arg768His and p.Asp926Glu) found in the three individuals occurred at evolutionary conserved amino acids (Figure 1B). Among the other candidate genes in individuals 1 and 3, *MSLN* (MIM 601051), encoding mesothelin isoform 1 preproprotein that is cleaved into megakaryocyte potentiating factor and mesothelin, is a potential candidate in the family of individual 1 as its homozygous variant segregated with the phenotype; however, it is expressed in epithelial mesotheliomas, and the mutation affects less conserved amino acid (Table S3). The other candidate genes' variants did not cosegregate with the phenotype. Thus, mutations in *POLR3B* are most likely to cause HCAHC in two families.

In individual 4, in whom no *POLR3B* mutations were found, there were six candidate genes for an autosomal-recessive model. Among them, *POLR3A* (MIM 614258, GenBank accession number NM_007055.3), harboring two missense mutations, appeared to be a primary candidate because it encodes the largest subunit of Pol III (RPC1) (Figure 1A and Table S2). By Sanger sequencing, we confirmed that a missense mutation (c.2690T>A [p.Ile897Asn]) in exon 20 was inherited from his father and that another missense mutation (c.3013C>T [p.Arg1005Cys]) in exon 23 was inherited from his mother (Figure 1A). The two mutations were not present in a healthy younger sister. The two missense mutations (p.Ile897Asn and p.Arg1005Cys) occurred at relatively conserved amino acids (Figure 1B). In total, we found four mutations in *POLR3B* and two mutations in *POLR3A*. Evaluation of the missense mutations by PolyPhen-2 program showed that three mutations (p.Arg768His,

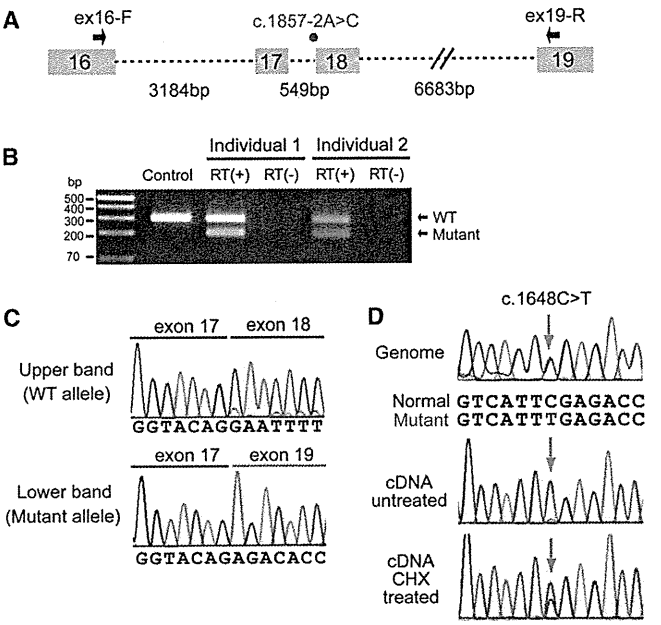

Figure 2. Effects of Splice-Site and Nonsense Mutations in *POLR3B*

(A) Schematic representation of the genomic structure of *POLR3B* from exon 16 to 19. Exons, introns, and primers are shown by boxes, dashed lines, and arrows, respectively. The mutation in intron 17 is depicted as a red dot.

(B) RT-PCR analysis of individuals 1 and 2 with c.1857-2A>C and a normal control. Two PCR products were detected from the individual's cDNA: the upper band is the wild-type (WT) transcript, and the lower band is the mutant. Only a single wild-type amplicon was detected in the control.

(C) Sequence of WT and mutant amplicons clearly showed exon 18 skipping in the mutant allele.

(D) Analysis of the c.1648C>T mutation. Sequence of PCR products amplified with genomic (upper), cDNA from untreated cells (middle), and cDNA from CHX treated cells (lower) as a template. Although untreated cells show extremely low levels of c.1648C>T mutant allele expression, cells treated to inhibit NMD show significantly increased levels of mutant allele expression.

p.Asp926Glu, and p.Ile897Asn) were probably damaging and that p.Arg1005Cys is tolerable. The c.2303G>A mutation (*POLR3B*) was found in one allele out of 540 Japanese control chromosomes. The remaining five mutations were not detected in 540 Japanese control chromosomes, indicating that the mutations are very rare in the Japanese population. Among the other candidate genes in individuals 4, *IGSF10*, a member of immunoglobulin superfamily, is a potential candidate because its variants segregated with the phenotype (Table S3); however, considering a close relationship between *POLR3A* and *POLR3B*, and the fact that *POLR3A* mutations have been recently reported in hypomyelinating leukodystrophy (see below),[12] *POLR3A* abnormality is the most plausible culprit for HCAHC in individual 4.

The structure of Pol III[13,14] and Pol II[15,16] is highly homologous, especially in the largest subunits. Thus, we extrapolated the mutations of RPC1 or RPC2 onto the structure of yeast Pol II (Protein Data Bank [PDB] accession number 3GTP)[17] (Figure 1C). RPB1 and RPB2 subunits of

yeast Pol II are homologous to RPC1 and RPC2 of Pol III, respectively. Asn620_Lys652 in RPC2 corresponds to Tyr679_Lys712 in RPB2. The deletion of Asn620_Lys652 (Tyr679_Lys712) would destroy a structural core of RPB2, leading to loss of RPB2 function. In addition, Arg768 (Arg852 in RPB2) interacts with the main-chain carbonyl group of Arg70 of the RPB12 subunit, and Asp926 (Asp1009 in RPB2) interacts with the side chain of Arg48 of the RPB10 subunit of Pol II (Figure 1D). Arg768His (Arg852His) and Asp926Glu (Asp1009Glu) substitutions are considered to disturb these subunit interactions, leading to dysfunction of the polymerase. Therefore, structural prediction suggests that the mutations in *POLR3B* (RPC2) could affect Pol III function. On the other hand, Ile897 and Arg1005 in RPC1 correspond to Val863 and Arg1036 in RPB1, respectively. Ile897 (Val863) has hydrophobic interactions with Leu170 and Pro176 of the RPB5 subunit and with Phe900 (Phe866) of the RPB1 subunit of Pol II (Figure 1E). Ile897Asn (Val863Asn) substitution is likely to disturb this interaction. Arg1005 (Arg1036) stabilizes interaction between RPB1 and RPB8 subunits (Figure 1F). The Arg1005Cys (Arg1036Cys) substitution appears to make this interaction unstable. Thus mutations in *POLR3A* are also predicted to affect Pol III function.

Clinical features of individuals with *POLR3A* or *POLR3B* mutations are presented in Table 1. MRI revealed high-intensity areas in the white matter in T2-weighted images, cerebellar atrophy, and a hypoplastic corpus callosum in all four individuals (Figure 3). Individuals 1 and 2 showed an extremely similar clinical course. They developed normally during their early infancy, i.e., walking unaided at 15 and 14 months, and uttering a few words at 12 and 13 months, respectively. After the age of 3, individual 1 presented with unstable walking and frequent stumbling and falling down, and individual 2 became poor at exercise. They both had severe myopia (corrected visual acuity of 0.7 and 0.5 at most, respectively). They graduated from elementary, junior high, and high schools with poor records, and the intelligence quotient (IQ) of individual 2 was 52 (WAIS-III). In individual 1, unstable walking was prominent at around 18 years, and he could not ride a bicycle because of ataxia; however, he could drive an automobile. Amenorrhea was noted in individual 2, and was successfully treated by hormone therapy. Individual 1 showed several signs of hypogonadism, including absence of underarm and mustache hair, thin pubic hair (Tanner II), and serum levels of testosterone, follicle stimulating hormone, and luteinizing hormone that were below normal for age 27. Neurological examination of both individuals revealed mild horizontal nystagmus, slowing of smooth-pursuit eye movement, and gaze limitation, especially in vertical gazing, hypotonia, mildly exaggerated deep-tendon reflex (patellar and Achilles tendon reflex) with negative Babinski reflex, and cerebellar signs and symptoms, including ataxic speech, wide-based ataxic gait, dysdiadochokinesis, and dysmetria. Clinical information for individual 3 has been reported previously.[6] Additional findings are as follows: slowing of smooth-pursuit eye movement, gaze limitation in vertical gazing, normal auditory brain responses (ABR), cerebral symptoms with mild spasticity, and intellectual disability (an IQ of 43 according to the WISC-III test), and no myopia but hypermetropic astigmatism. She showed no deterioration besides a mild dysphagia and walks herself to a school for the disabled. Individual 4 developed normally during his

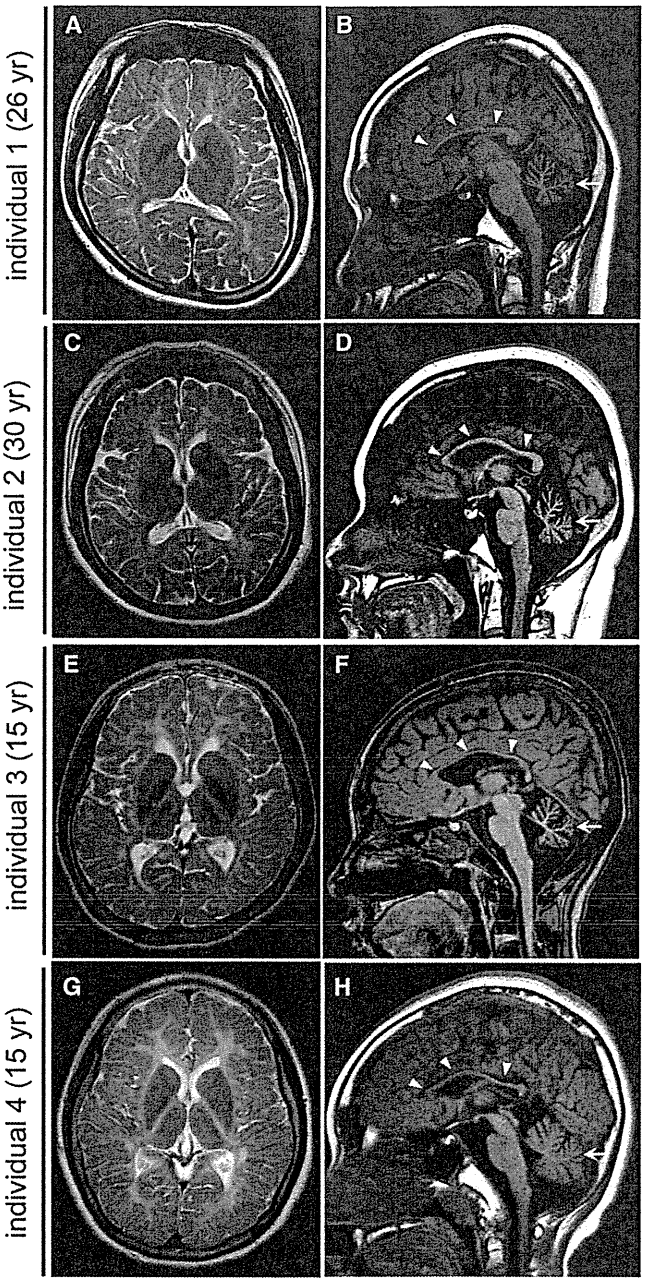

Figure 3. Brain MRI of Individuals with *POLR3B* and *POLR3A* Mutations

(A, C, E, and G) T2-weighted axial images through the basal ganglia. High-intensity areas in the white matter were observed in all individuals.

(B, D, F, and H) T1-weighted midline sagittal images. All the individuals showed hypoplastic corpus callosum (arrowheads) and atrophy of cerebellum (arrows).

early infancy, had normal head control at 3 months, was speaking a few words at 12 months, and was walking unaided at 14 months. His parents noted mild tremors around 4 years. He had normal stature, weight, and head circumference. Although he had severe myopia, his eye movement was smooth with no limitation or nystagmus. He had sensory neuronal deafness on the left side. He showed normal muscle tone and had no spasticity or rigidity. His tendon reflexes were slightly elevated with a negative Babinski reflex. Cerebellar signs were noted; expressive ataxic explosive speech, intension tremor, poor finger to nose test, dysdiadochokinesis, dysmetria, and wide-based ataxic gait. His intelligence quotient was 57 (according to the WISC-III test). His peripheral nerve conduction velocity was within the normal range and his ABR showed normal responses on the right side. He suffered motor deterioration around age 14 and became wheelchair bound.

In this study, we successfully identified compound heterozygous mutations in *POLR3A* and *POLR3B* in individuals with HCAHC. Very recently, Bernard et al.[12] reported that *POLR3A* mutations cause three overlapping leukodystrophies, including 4H syndrome, suggesting that HCAHC is, at least in part, within a wide clinical spectrum caused by *POLR3A* mutations. The p.Arg1005Cys mutation was shared between individual 9 in their report and our individual 4. All 19 individuals with *POLR3A* mutations showed progressive upper motor neuron dysfunction and cognitive regression. In addition, individual 9 showed abnormal eye movement, hypodontia, and hypogonadism. None of these features were recognized in our individual 4; these differences further support phenotypic variability of *POLR3A* mutations.[12] Given the phenotypic similarities among 4H syndrome, HCAHC, and H-ABC, there is a possibility that H-ABC is also allelic and caused by recessive mutations in either *POLR3A* or *POLR3B*.

Pol III consists of 17 subunits and is involved in the transcription of small noncoding RNAs, such as 5S ribosomal RNA (rRNA), U6 small nuclear RNA (snRNA), 7SL RNA, RNase P, RNase MRP, short interspersed nuclear elements (SINEs), and all transfer RNAs (tRNAs). Pol III-transcribed genes are classified into three types based on promoter elements and transcription factors. 5S rRNA is a solo type I gene. Type II genes include tRNA, 7SL RNA, and SINEs. Type III genes include U6 snRNA, RNase P, and RNase MRP.[18–20] The Pol III system is important for cell growth in yeast, and its transcription is tightly regulated during the cell cycle.[20] In zebrafish, *polr3b* mutant larvae that have a deletion of 41 conserved amino acids (Δ239-279) from the Rpc2 protein showed a proliferation deficit in multiple tissues, including intestine, endocrine pancreas, liver, retina and terminal branchial arches.[21] In the mutants, the expression levels of tRNA were significantly reduced, whereas the level of 5S rRNA expression was not changed, suggesting that this *polr3b* mutation can differentially affect Pol III target promoters.[21] RPC2 contributes to the catalytic activity of the polymerase and forms the active center of the polymerase together with the largest subunit, RPC1.[22] Thus, it is reasonable to consider that mutations in *POLR3A* and *POLR3B* cause overlapping phenotypes. Indeed, three individuals with *POLR3B* mutations showed diffuse cerebral hypomyelination, atrophy of the cerebellum and corpus callosum, and abnormal eye movements that overlap with *POLR3A* abnormalities.[12] Furthermore, two out of three individuals showed hypogonadism, suggesting a common pathological mechanism between *POLR3A* and *POLR3B* mutations. In the zebrafish *polr3b* mutants there were no defects of the central nervous system other than a reduced size of the retina, probably reflecting species differences; however, the reduced level of tRNA in the *polr3b* mutants raises the possibility that defects of tRNA transcription by Pol III could be a common pathological mechanism underlying *POLR3A* and *POLR3B* mutations. Supporting this idea, mutations in two genes involved in aminoacylation activity of tRNA synthetase cause defects of myelination in central nervous system: *DARS2* (MIM 610956) and *AIMP* (MIM 603605).[23,24] In addition, mutations in four genes encoding aminoacyl-tRNA synthetase cause Charcot-Marie-Tooth disease (MIM 613641, 613287, 601472, and 608323), resulting from demyelination of peripheral nerve axons: *KARS* (MIM 601421), *GARS* (MIM 600287), *YARS* (MIM 603623), and *AARS* (MIM 601065).[25–28] Thus, it is very likely that regulation of tRNA expression is essential for development and maintenance of myelination in both central and peripheral nervous systems.

An interesting clinical feature of *POLR3B* mutations is the absence of motor deterioration. All three individuals with *POLR3B* mutations could walk without support at ages 16, 27, and 30, whereas individual 3 with *POLR3A* mutations had motor deterioration around age 14. Bernard et al.[12] also reported progressive upper motor neuron dysfunction and cognitive regression in individuals with *POLR3A* mutations. Thus, there is a possibility that phenotypes caused by *POLR3A* mutations could be more severe and progressive than *POLR3B* mutant phenotypes. Identification of a greater number of cases with *POLR3B* mutations is required to confirm this hypothesis.

In conclusion, our data, together with that of a previous report,[12] demonstrate that mutations in Pol III subunits cause overlapping autosomal-recessive hypomyelinating disorders. Establishment of an animal model will facilitate our understanding of the pathophysiology of the multiple defects caused by Pol III mutations.

Supplemental Data

Supplemental Data include three tables and can be found with this article online at http://www.cell.com/AJHG/.

Acknowledgments

We would like to thank all the individuals and their families for their participation in this study. This work was supported by

research grants from the Ministry of Health, Labour, and Welfare (H.S., H.O., M.S., J.T., N. Miyake, K.I. and N. Matsumoto), the Japan Science and Technology Agency (N. Matsumoto), a Grant-in-Aid for Scientific Research on Innovative Areas (Foundation of Synapse and Neurocircuit Pathology) from the Ministry of Education, Culture, Sports, Science and Technology of Japan (N. Matsumoto), a Grant-in-Aid for Scientific Research from Japan Society for the Promotion of Science (H.O., N. Matsumoto), a Grant-in-Aid for Young Scientist from Japan Society for the Promotion of Science (H.S.). This work has been done at Advanced Medical Research Center, Yokohama City University.

Received: August 31, 2011
Revised: October 5, 2011
Accepted: October 10, 2011
Published online: October 27, 2011

Web Resources

The URLs for data presented herein are as follows:

ClustalW, http://www.genome.jp/tools/clustalw/
dbSNP, http://www.ncbi.nlm.nih.gov/projects/SNP/
Ensembl, http://uswest.ensembl.org/index.html
GenBank, http://www.ncbi.nlm.nih.gov/Genbank/
Online Mendelian Inheritance in Man, http://www.omim.org
PolyPhen-2, http://genetics.bwh.harvard.edu/pph2/
Protein Data Bank, http://www.pdb.org/pdb/home/home.do
PyMOL, http://www.pymol.org/
SeattleSeq Annotation, http://gvs.gs.washington.edu/SeattleSeq Annotation/

References

1. Schiffmann, R., and van der Knaap, M.S. (2009). Invited article: an MRI-based approach to the diagnosis of white matter disorders. Neurology *72*, 750–759.
2. Timmons, M., Tsokos, M., Asab, M.A., Seminara, S.B., Zirzow, G.C., Kaneski, C.R., Heiss, J.D., van der Knaap, M.S., Vanier, M.T., Schiffmann, R., and Wong, K. (2006). Peripheral and central hypomyelination with hypogonadotropic hypogonadism and hypodontia. Neurology *67*, 2066–2069.
3. Wolf, N.I., Harting, I., Boltshauser, E., Wiegand, G., Koch, M.J., Schmitt-Mechelke, T., Martin, E., Zschocke, J., Uhlenberg, B., Hoffmann, G.F., et al. (2005). Leukoencephalopathy with ataxia, hypodontia, and hypomyelination. Neurology *64*, 1461–1464.
4. Wolf, N.I., Harting, I., Innes, A.M., Patzer, S., Zeitler, P., Schneider, A., Wolff, A., Baier, K., Zschocke, J., Ebinger, F., et al. (2007). Ataxia, delayed dentition and hypomyelination: a novel leukoencephalopathy. Neuropediatrics *38*, 64–70.
5. van der Knaap, M.S., Naidu, S., Pouwels, P.J., Bonavita, S., van Coster, R., Lagae, L., Sperner, J., Surtees, R., Schiffmann, R., and Valk, J. (2002). New syndrome characterized by hypomyelination with atrophy of the basal ganglia and cerebellum. AJNR Am. J. Neuroradiol. *23*, 1466–1474.
6. Sasaki, M., Takanashi, J., Tada, H., Sakuma, H., Furushima, W., and Sato, N. (2009). Diffuse cerebral hypomyelination with cerebellar atrophy and hypoplasia of the corpus callosum. Brain Dev. *31*, 582–587.
7. Li, H., Ruan, J., and Durbin, R. (2008). Mapping short DNA sequencing reads and calling variants using mapping quality scores. Genome Res. *18*, 1851–1858.
8. Doi, H., Yoshida, K., Yasuda, T., Fukuda, M., Fukuda, Y., Morita, H., Ikeda, S., Kato, R., Tsurusaki, Y., Miyake, N., et al. (2011). Exome sequencing reveals a homozygous *SYT14* mutation in adult-onset, autosomal-recessive spinocerebellar ataxia with psychomotor retardation. Am. J. Hum. Genet. *89*, 320–327.
9. Pierce, S.B., Walsh, T., Chisholm, K.M., Lee, M.K., Thornton, A.M., Fiumara, A., Opitz, J.M., Levy-Lahad, E., Klevit, R.E., and King, M.C. (2010). Mutations in the DBP-deficiency protein HSD17B4 cause ovarian dysgenesis, hearing loss, and ataxia of Perrault Syndrome. Am. J. Hum. Genet. *87*, 282–288.
10. Gilissen, C., Arts, H.H., Hoischen, A., Spruijt, L., Mans, D.A., Arts, P., van Lier, B., Steehouwer, M., van Reeuwijk, J., Kant, S.G., et al. (2010). Exome sequencing identifies *WDR35* variants involved in Sensenbrenner syndrome. Am. J. Hum. Genet. *87*, 418–423.
11. Saitsu, H., Kato, M., Okada, I., Orii, K.E., Higuchi, T., Hoshino, H., Kubota, M., Arai, H., Tagawa, T., Kimura, S., et al. (2010). *STXBP1* mutations in early infantile epileptic encephalopathy with suppression-burst pattern. Epilepsia *51*, 2397–2405.
12. Bernard, G., Chouery, E., Putorti, M.L., Tetreault, M., Takanohashi, A., Carosso, G., Clement, I., Boespflug-Tanguy, O., Rodriguez, D., Delague, V., et al. (2011). Mutations of *POLR3A* Encoding a Catalytic Subunit of RNA Polymerase Pol III Cause a Recessive Hypomyelinating Leukodystrophy. Am. J. Hum. Genet. *89*, 415–423.
13. Jasiak, A.J., Armache, K.J., Martens, B., Jansen, R.P., and Cramer, P. (2006). Structural biology of RNA polymerase III: subcomplex C17/25 X-ray structure and 11 subunit enzyme model. Mol. Cell *23*, 71–81.
14. Fernández-Tornero, C., Böttcher, B., Riva, M., Carles, C., Steuerwald, U., Ruigrok, R.W., Sentenac, A., Müller, C.W., and Schoehn, G. (2007). Insights into transcription initiation and termination from the electron microscopy structure of yeast RNA polymerase III. Mol. Cell *25*, 813–823.
15. Cramer, P., Bushnell, D.A., and Kornberg, R.D. (2001). Structural basis of transcription: RNA polymerase II at 2.8 angstrom resolution. Science *292*, 1863–1876.
16. Gnatt, A.L., Cramer, P., Fu, J., Bushnell, D.A., and Kornberg, R.D. (2001). Structural basis of transcription: an RNA polymerase II elongation complex at 3.3 A resolution. Science *292*, 1876–1882.
17. Wang, D., Bushnell, D.A., Huang, X., Westover, K.D., Levitt, M., and Kornberg, R.D. (2009). Structural basis of transcription: backtracked RNA polymerase II at 3.4 angstrom resolution. Science *324*, 1203–1206.
18. Oler, A.J., Alla, R.K., Roberts, D.N., Wong, A., Hollenhorst, P.C., Chandler, K.J., Cassiday, P.A., Nelson, C.A., Hagedorn, C.H., Graves, B.J., and Cairns, B.R. (2010). Human RNA polymerase III transcriptomes and relationships to Pol II promoter chromatin and enhancer-binding factors. Nat. Struct. Mol. Biol. *17*, 620–628.
19. Dieci, G., Fiorino, G., Castelnuovo, M., Teichmann, M., and Pagano, A. (2007). The expanding RNA polymerase III transcriptome. Trends Genet. *23*, 614–622.
20. Dumay-Odelot, H., Durrieu-Gaillard, S., Da Silva, D., Roeder, R.G., and Teichmann, M. (2010). Cell growth- and differentiation-dependent regulation of RNA polymerase III transcription. Cell Cycle *9*, 3687–3699.

21. Yee, N.S., Gong, W., Huang, Y., Lorent, K., Dolan, A.C., Maraia, R.J., and Pack, M. (2007). Mutation of RNA Pol III subunit *rpc2/polr3b* Leads to Deficiency of Subunit Rpc11 and disrupts zebrafish digestive development. PLoS Biol. *5*, e312.
22. Werner, M., Thuriaux, P., and Soutourina, J. (2009). Structure-function analysis of RNA polymerases I and III. Curr. Opin. Struct. Biol. *19*, 740–745.
23. Scheper, G.C., van der Klok, T., van Andel, R.J., van Berkel, C.G., Sissler, M., Smet, J., Muravina, T.I., Serkov, S.V., Uziel, G., Bugiani, M., et al. (2007). Mitochondrial aspartyl-tRNA synthetase deficiency causes leukoencephalopathy with brain stem and spinal cord involvement and lactate elevation. Nat. Genet. *39*, 534–539.
24. Feinstein, M., Markus, B., Noyman, I., Shalev, H., Flusser, H., Shelef, I., Liani-Leibson, K., Shorer, Z., Cohen, I., Khateeb, S., et al. (2010). Pelizaeus-Merzbacher-like disease caused by AIMP1/p43 homozygous mutation. Am. J. Hum. Genet. *87*, 820–828.
25. Latour, P., Thauvin-Robinet, C., Baudelet-Méry, C., Soichot, P., Cusin, V., Faivre, L., Locatelli, M.C., Mayençon, M., Sarcey, A., Broussolle, E., et al. (2010). A major determinant for binding and aminoacylation of tRNA(Ala) in cytoplasmic Alanyl-tRNA synthetase is mutated in dominant axonal Charcot-Marie-Tooth disease. Am. J. Hum. Genet. *86*, 77–82.
26. McLaughlin, H.M., Sakaguchi, R., Liu, C., Igarashi, T., Pehlivan, D., Chu, K., Iyer, R., Cruz, P., Cherukuri, P.F., Hansen, N.F., et al. (2010). Compound heterozygosity for loss-of-function lysyl-tRNA synthetase mutations in a patient with peripheral neuropathy. Am. J. Hum. Genet. *87*, 560–566.
27. Antonellis, A., Ellsworth, R.E., Sambuughin, N., Puls, I., Abel, A., Lee-Lin, S.Q., Jordanova, A., Kremensky, I., Christodoulou, K., Middleton, L.T., et al. (2003). Glycyl tRNA synthetase mutations in Charcot-Marie-Tooth disease type 2D and distal spinal muscular atrophy type V. Am. J. Hum. Genet. *72*, 1293–1299.
28. Jordanova, A., Irobi, J., Thomas, F.P., Van Dijck, P., Meerschaert, K., Dewil, M., Dierick, I., Jacobs, A., De Vriendt, E., Guergueltcheva, V., et al. (2006). Disrupted function and axonal distribution of mutant tyrosyl-tRNA synthetase in dominant intermediate Charcot-Marie-Tooth neuropathy. Nat. Genet. *38*, 197–202.

REPORT

Exome Sequencing Reveals a Homozygous *SYT14* Mutation in Adult-Onset, Autosomal-Recessive Spinocerebellar Ataxia with Psychomotor Retardation

Hiroshi Doi,[1,2] Kunihiro Yoshida,[3] Takao Yasuda,[4] Mitsunori Fukuda,[4] Yoko Fukuda,[5] Hiroshi Morita,[6] Shu-ichi Ikeda,[6] Rumiko Kato,[7] Yoshinori Tsurusaki,[1] Noriko Miyake,[1] Hirotomo Saitsu,[1] Haruya Sakai,[1] Satoko Miyatake,[1] Masaaki Shiina,[8] Nobuyuki Nukina,[9] Shigeru Koyano,[2] Shoji Tsuji,[5] Yoshiyuki Kuroiwa,[2] and Naomichi Matsumoto[1,*]

Autosomal-recessive cerebellar ataxias (ARCAs) are clinically and genetically heterogeneous disorders associated with diverse neurological and nonneurological features that occur before the age of 20. Currently, mutations in more than 20 genes have been identified, but approximately half of the ARCA patients remain genetically unresolved. In this report, we describe a Japanese family in which two siblings have slow progression of a type of ARCA with psychomotor retardation. Using whole-exome sequencing combined with homozygosity mapping, we identified a homozygous missense mutation in *SYT14*, encoding synaptotagmin XIV (SYT14). Expression analysis of the mRNA of *SYT14* by a TaqMan assay confirmed that *SYT14* mRNA was highly expressed in human fetal and adult brain tissue as well as in the mouse brain (especially in the cerebellum). In an in vitro overexpression system, the mutant SYT14 showed intracellular localization different from that of the wild-type. An immunohistochemical analysis clearly showed that SYT14 is specifically localized to Purkinje cells of the cerebellum in humans and mice. Synaptotagmins are associated with exocytosis of secretory vesicles (including synaptic vesicles), indicating that the alteration of the membrane-trafficking machinery by the *SYT14* mutation may represent a distinct pathomechanism associated with human neurodegenerative disorders.

Hereditary ataxias are genetically heterogeneous neurological disorders: autosomal-dominant, autosomal-recessive, X-linked, and mitochondrial types are known. Among ataxias, spinocerebellar ataxia (SCA) is relatively common and involves the cerebellum, brainstem, or spinocerebellar long tracts.[1] Autosomal-recessive cerebellar ataxias (ARCAs) are generally associated with diverse neurological and nonneurological attributes, resulting in complex phenotypes. ARCAs include congenital nonprogressive ataxias and progressive ataxias such as SCAs.[2] The clinical onset of ARCAs usually occurs before the age of 20, even if congenital types are excluded.[1,3,4] Currently, more than 20 defective genes have been identified in ARCAs.[2,5,6] These genes have variable recognized functions, including those involving mitochondrial energy generation, cellular metabolisms, DNA repair, chaperone-mediated protein folding, RNA processing, and ion channels.[1,3,6] Approximately half of the patients with ARCAs remain genetically unresolved.[4] Therefore, more investigations of ARCAs are required. In this study, we describe a Japanese family with two siblings showing psychomotor retardation and the slowly progressive type of SCA without involvement of pyramidal tracts or peripheral nerves. Exome sequencing combined with homozygosity mapping successfully identified a causative mutation.

Clinical information and blood materials were obtained from the family members after written informed consent was secured. Experimental protocols were approved by IRBs of the Yokohama City University and the Shinshu University. Among the children of first-cousin parents, two siblings (IV-3 and IV-4) were found to be affected, whereas the other two (IV-1 and IV-2) were healthy (Figure 1A). No similar patients were recognized within the family. IV-3 had mild psychomotor retardation from childhood. He found a job after graduating from an ordinary junior high school. At 35 years of age, he lost his job for social reasons. Although he had some gait disturbances from childhood, he could independently go shopping and walk a dog even after leaving his occupation. At the age of ~56, he developed obvious gait unsteadiness and began to stumble frequently. At 58, he started to choke on food. These symptoms gradually worsened, and he sought medical examination at 59 years of age. He displayed disturbances of smooth-pursuit eye movements, dysarthria, mild limb ataxia, and moderate truncal ataxia. His muscle tone was normal, and no involuntary

[1]Department of Human Genetics, Graduate School of Medicine, Yokohama City University, 3-9 Fukuura, Kanazawa-ku, Yokohama 236-0004, Japan; [2]Department of Clinical Neurology and Stroke Medicine, Graduate School of Medicine, Yokohama City University, 3-9 Fukuura, Kanazawa-ku, Yokohama 236-0004, Japan; [3]Division of Neurogenetics, Department of Brain Disease Reseach, Shinshu University School of Medicine, 3-1-1 Asahi, Matsumoto, Nagano 390-8621, Japan; [4]Laboratory of Membrane Trafficking Mechanisms, Department of Developmental Biology and Neuroscience, Graduate School of Life Sciences, Tohoku University, Aobayama, Aoba-ku, Sendai, Miyagi 980-8578, Japan; [5]Department of Neurology, Graduate School of Medicine, The University of Tokyo, 7-3-1 Hongo, Bunkyo-ku, Tokyo 113-8655, Japan; [6]Department of Medicine (Neurology & Rheumatology), Shinshu University School of Medicine, 3-1-1 Asahi, Matsumoto, Nagano 390-8621, Japan; [7]Department of Pediatrics, National Higashi-Saitama Hospital, 4147 Kurohama, Hasuda 349-0196, Japan; [8]Department of Biochemistry, Graduate School of Medicine, Yokohama City University, 3-9 Fukuura, Kanazawa-ku, Yokohama 236-0004, Japan; [9]Laboratory for Structural Neuropathology, Brain Science Institute, RIKEN, 2-1 Hirosawa, Wako 351-0198, Japan
*Correspondence: naomat@yokohama-cu.ac.jp
DOI 10.1016/j.ajhg.2011.07.012.